

# A Water-Soluble Pillar[6]arene: Synthesis, Host–Guest Chemistry, and Its Application in Dispersion of Multiwalled Carbon Nanotubes in Water

Guocan Yu, Min Xue, Zibin Zhang, Jinying Li, Chengyou Han, and Feihe Huang\*

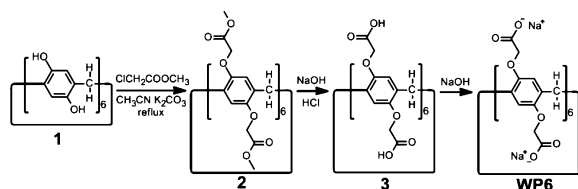
MOE Key Laboratory of Macromolecular Synthesis and Functionalization, Department of Chemistry, Zhejiang University, Hangzhou 310027, P. R. China

## Supporting Information

**ABSTRACT:** The first water-soluble pillar[6]arene was synthesized. Its water solubility can be reversibly controlled by changing the pH. This solubility control was used in reversible transformations between nanotubes and vesicles and dispersion of multiwalled carbon nanotubes in water.

Macrocycles such as crown ethers,<sup>1</sup> cyclodextrins,<sup>2</sup> calixarenes,<sup>3</sup> and cucurbiturils<sup>4</sup> have attracted much interest because of their applications in a broad range of fields, including memory storage, smart supramolecular polymers, drug delivery systems, sensors, protein probes, and functional nanodevices.<sup>5</sup> Pillar[*n*]arenes, mainly including pillar[5]arenes<sup>6</sup> and pillar[6]arenes,<sup>7</sup> are new macrocyclic hosts made up of hydroquinone units linked by methylene (–CH<sub>2</sub>–) bridges at their 2- and 5-positions. Their syntheses, conformational mobility, derivatization, host–guest complexation with different guests, and self-assembly have recently been actively explored.<sup>6,7</sup> With the current emphasis on “environment-friendly chemistry”, the search for water-soluble hosts that could accommodate water-insoluble guest molecules within their confined hydrophobic cavities has gained momentum.<sup>8</sup> Water-soluble pillar[5]arenes have been demonstrated to have interesting host–guest chemistry.<sup>6c,i,k</sup> In this work, the first water-soluble pillar[6]arene, **WP6**, was synthesized by introducing carboxylate anionic groups on both rims (Scheme 1). By etherification of **1**,<sup>7e</sup> methox-

## Scheme 1. Synthetic Route to WP6



ycarbonylmethoxy-substituted pillar[6]arene **2** was synthesized. The hydrolysis of **2** under basic conditions afforded carboxylic acid-substituted pillar[6]arene **3**. By treatment with 1 equiv of sodium hydroxide in aqueous solution, water-soluble pillar[6]arene **WP6** was obtained.

**WP6** strongly binds organic pyridinium salt **G1** in water, mainly driven by hydrophobic and electrostatic interactions. Successful manipulation of self-assembling nanostructures was

achieved by noncovalent modification of this amphiphilic guest with the water-soluble pillar[6]arene host, which caused a transformation from nanotubes to vesicles. Adjusting the pH to make the solution acidic protonates the carboxylate groups on both rims of the pillar[6]arene, affording insoluble carboxylic acid groups. On the contrary, by increasing the pH value, the –COOH units are deprotonated again. Therefore, the solubility of the pillar[6]arene can be reversibly controlled just by changing the pH of the solution, resulting in the reversible transformation of the host–guest system between nanotubes and vesicles. Furthermore, its confined hydrophobic cavity was utilized to interact with neutral guest molecule **G2** through hydrophobic interactions. This host–guest system can be used in pH-controlled reversible dispersion of multiwalled carbon nanotubes (MWNTs) in water, improving their applications in many fields, such as controllable nanocatalysis and controllable nanocarriers.

The pH-responsiveness of **WP6** was verified by fluorescence experiments. The fluorescence intensity at 330 nm corresponding to the characteristic peak for **WP6** was almost unchanged when the solution pH was changed from 10.5 to 7.3 but decreased rapidly when the solution pH was changed from 7.3 to 6.8. On the other hand, no significant intensity changes were observed when the pH was decreased from 6.8 to 2.6 (Figure S16 in the Supporting Information). The opposite phenomena were observed when the pH was increased from 2.5 to 10.6 (Figure S17). The pH-controlled solubility of **WP6** was also confirmed using <sup>1</sup>H NMR spectroscopy. Proton signals from **WP6** (1.00 mM) could be easily collected, but when the water-soluble host precipitated from D<sub>2</sub>O after acidification of the solution, the signals disappeared. When the solution was made basic, the precipitated host redissolved in the solution, and the <sup>1</sup>H NMR signals reappeared. These results showed that the solubility of the pillar[6]arene could be easily controlled simply by changing the pH.

To investigate higher-order self-assembled aggregates in water, an aqueous solution of **G1** was prepared with a concentration of 1.00 × 10<sup>−4</sup> M, which is higher than its critical aggregation concentration (CAC). As indicated by transmission electron microscopy (TEM) (Figure 1a), regular nanotubes were observed with an average diameter of ~300 nm. Interestingly, upon addition of 1 equiv of **WP6**, vesicles with a diameter of ~300 nm were observed (Figure 1b), drastically different from

Received: July 1, 2012

Published: July 24, 2012

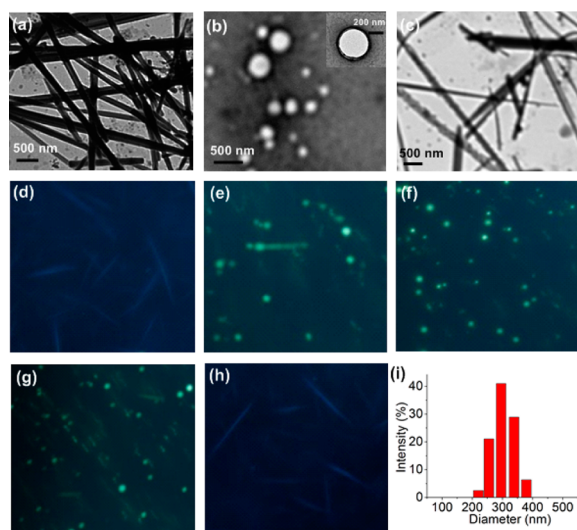


**Figure 1.** (a–c) TEM images of (a) G1 aggregates, (b) WP6⊃G1 aggregates, and (c) WP6⊃G1 aggregates after the solution pH was adjusted to 6.0. (d–h) Fluorescence microscopy images ( $10\ \mu\text{m} \times 10\ \mu\text{m}$ ) of (d) G1 aggregates, (e) 5 s and (f) 10 s after addition of 1 equiv of WP6, and (g) 10 s and (h) 30 s after the solution pH was adjusted to 6.0. (i) DLS data of WP6⊃G1 aggregates at pH >7.0.

the hollow nanotubes formed by G1 alone. These regular nanotubes with the same diameter reappeared when the solution pH was adjusted to 6.0 (Figure 1c). We also used fluorescence microscopy to monitor the changes in the self-assembled structures (Figure 1d–h). Tubular assemblies formed by G1 could be clearly seen (Figure 1d). Upon addition of WP6, the self-assembled nanotubes of G1 were rapidly transformed into vesicles. It took  $\sim 10$  s to transform the nanotubes into vesicles completely. When the solution pH was adjusted to acidity, the WP6⊃G1 vesicles were gradually transformed back into nanotubes. Moreover, when the pH was higher than 7.0, vesicles rather than nanotubes formed in solution. Therefore, the self-assembly of this host–guest system could be reversibly controlled between nanotubes and vesicles by changing the pH. As shown by dynamic light scattering (DLS), the main diameter distribution of the WP6⊃G1 vesicles was  $\sim 312$  nm (Figure 1i), in good agreement with the TEM image in Figure 1b.

The packing of G1 in the nanotubes (Figure 2) was studied by UV–vis spectroscopy and X-ray diffraction (XRD). The blue shift upon dilution (Figure 3a) indicated an H-aggregation form,<sup>9</sup> suggesting that adjacent pyrene aromatic rings undergo considerable overlap through  $\pi$ – $\pi$  stacking interactions (Figure 2). The bilayer structure of the membrane was confirmed by XRD and small-angle X-ray scattering (SAXS). The bilayer thickness bilayer was calculated to be 4.8 nm (Figure S19a), which is equal to the length of two G1 molecules with antiparallel packing and overlapped pyrene rings (Figure 2).

We then investigated whether the bilayer structure was damaged after complexation. It was verified by XRD and SAXS that the structure was retained with a bilayer thickness of  $\sim 4.8$  nm after complexation (Figure S19b). A mechanism is proposed to explain why the shape of the G1 aggregates is transformed from nanotubes to vesicles after complexation with WP6 (Figure 2). The microassembled structure of the aggregates formed by the two distinct bilayers is determined by the curvature of the membrane. Typically, high membrane curvature favors nanotubular structures, while a vesicular structure is dependent on a low-curvature membrane.<sup>51</sup> Prior to complexation with WP6, G1

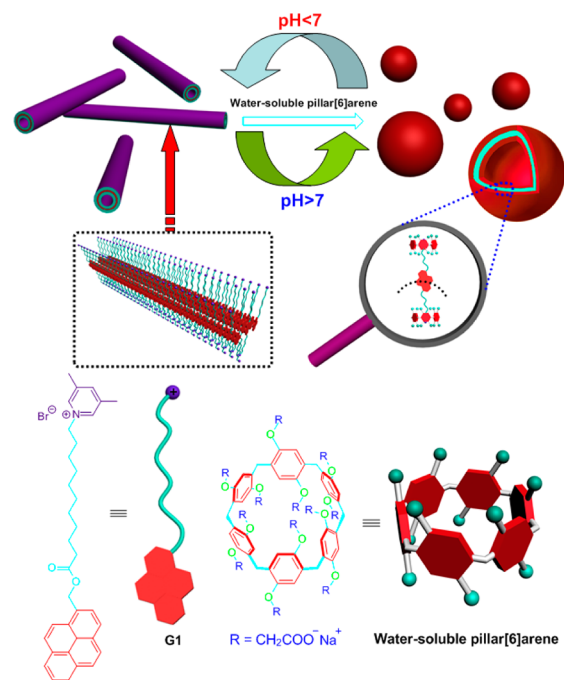


**Figure 2.** Schematic representations of (top) the reversible transformations between G1 nanotubes and WP6⊃G1 vesicles and (bottom) the molecular structures of WP6 and G1.

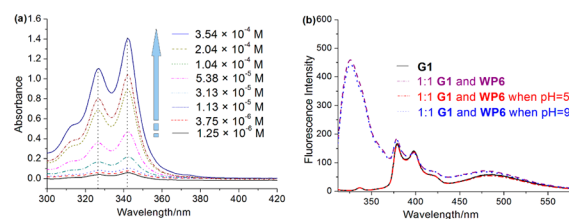


**Figure 3.** (a) UV–vis absorption spectra of aqueous solutions of G1 at different concentrations. (b) Fluorescence emission spectra of G1 and WP6⊃G1 at WP6 and G1 concentrations of  $4.00 \times 10^{-5}$  M.

self-assembles in aqueous solution to form a highly ordered bilayer of pyrenyl groups through  $\pi$ – $\pi$  stacking interactions, generating high curvature and forming a tubular structure (Figure 2). Upon complexation, WP6 is inserted into the membrane of the G1 nanotubes to form 1:1 [2]pseudorotaxanes through hydrophobic and electrostatic interactions without changing the thickness of the membrane. Because of the steric hindrance and the electrostatic repulsion generated upon insertion of the WP6 molecules, the straight G1 arrays along the axis become curved, resulting in the formation of a vesicular structure with low curvature (Figure 2). As WP6 precipitates from water after acidification of the solution, G1 dethreads from the cavity of the host and forms nanotubes again. This structural transformation from nanotubes to vesicles was revealed through fluorescence microscopy (Figure 1d–h). Figure 1e reveals the coexistence of nanotubes and vesicles upon addition of WP6, indicating a nanotube-to-vesicle transformation. The nanotubes disappeared completely within  $\sim 10$  s after addition of WP6, being replaced by vesicular structures. It should also be noted that a typical intermediate state between vesicles and nanotubes could also be observed by adjusting the solution pH to 6.0 (Figure 1g), supporting the mechanism mentioned above.

The complexation of G1 with WP6 was further studied by  $^1\text{H}$  NMR spectroscopy. Because of the relatively poor solubility of

**G1** in water, 1-octylpyridinium bromide (**OPB**) was used as a model compound. Upon addition of **WP6**, significant chemical shift changes of the **OPB** protons appeared (Figure S20), providing strong evidence of **WP6**–**OPB** interactions. Also, a mole ratio plot based on fluorescence titrations (Figure S22) showed that the complex formed by **WP6** and **OPB** has 1:1 stoichiometry, and the association constant ( $K_a$ ) in water was calculated to be  $(3.26 \pm 0.28) \times 10^5 \text{ M}^{-1}$  using a nonlinear curve-fitting method (Figure S23).

Further evidence for the formation of **WP6**⊃**G1** was obtained from UV–vis absorption spectroscopy. Upon addition of 1 equiv of **WP6**, the spectrum exhibited a broad absorption above 400 nm that corresponds to the characteristic absorption of the charge-transfer complex.<sup>10</sup> On the other hand, a notable red shift was observed (Figure S24), which indicated electronic communication between **WP6** and **G1**. Fluorescence spectra (Figure 3b) showed that making the solution acidic changed the water-soluble  $-\text{COO}^-$  groups of **WP6** to insoluble  $-\text{COOH}$  groups, resulting in the decomplexation of **WP6**⊃**G1**. However, this 1:1 [2]pseudorotaxane formed again when the solution was made basic, and this process could be reversibly cycled many times (Figure S25).

Carbon nanotubes (CNTs) have been the subject of great interest because of their extraordinary electronic, mechanical, and adsorption properties and applications in diverse areas of nanoscience.<sup>11</sup> However, their lack of solubility in solvents presents a considerable impediment to harnessing their applications. Noncovalent supramolecular approaches to functionalize the sidewalls of CNTs can preserve their unique properties.<sup>12</sup> Among these approaches based on noncovalent interactions, easily prepared pyrene derivatives with a large variety of functional groups have been used to solubilize the CNTs through  $\pi$ – $\pi$  interactions.<sup>11b</sup> The interaction with pyrene molecules partially exfoliates the CNT bundles and brings individual tubes into solution. These supramolecular approaches do not form any covalent bonds but instead form only  $\pi$ – $\pi$  interactions and thus only weakly perturb the nanotube conjugated system. In these systems, the solubility of the CNTs is hard to control, resulting in the limitation of their application to some degree. Here we used the confined hydrophobic cavity of **WP6** to interact with a neutral guest **G2** containing a  $\pi$ -rich pyrenyl ring through hydrophobic interactions. As shown in Figure S26, the association constant between **WP6** and **G2** was estimated to be  $(8.04 \pm 0.68) \times 10^4 \text{ M}^{-1}$  using the Stern–Volmer equation.<sup>13</sup> The solubility of this host–guest system can be controlled by adjusting the pH of the solution. Therefore, the solubility of the MWNTs can be controlled easily, and this process can also be achieved reversibly.

We found that MWNTs were dispersed very well in an aqueous solution of **WP6**⊃**G2** through simple sonication but could not be dispersed by **G2** alone. The black solution of the **WP6**⊃**G2**/MWNT complex was homogeneous and stable (Figure 4) and could stand for >1 month without significant change. This observation indicates that **WP6**⊃**G2** plays an important role in the solubilization of MWNTs. Moreover, MWNTs precipitated when the solution pH was made acidic and could be dispersed in water again when the solution pH was raised above 7.0. Thus, this dispersion could be reversibly controlled simply by changing the solution pH.

Direct evidence for **WP6**⊃**G2**–MWNT interactions was obtained using TEM and scanning electron microscopy (SEM). TEM images of pristine MWNTs showed the presence of large aggregates of nanotubes (Figure 4a). Upon addition of

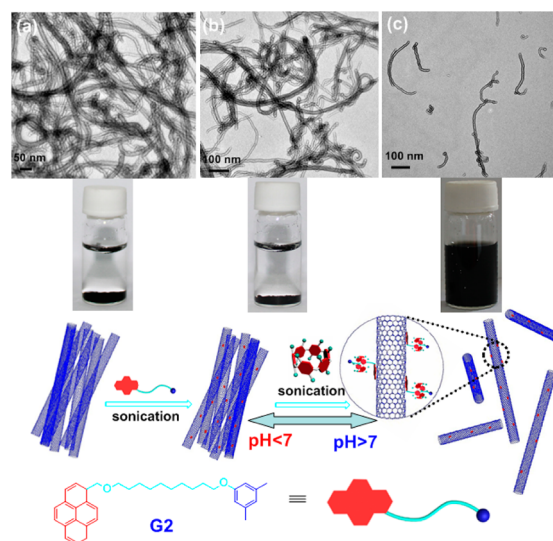


**Figure 4.** (top) TEM images of (a) MWNTs, (b) **G2** and MWNTs, and (c) **WP6**⊃**G2**/MWNT complexes and photographs of the corresponding mixtures with water. (bottom) Illustration of the pH-responsive solubility of the MWNTs in the presence of **WP6**⊃**G2**.

**G2**, no changes occurred, and the MWNTs were still aggregated (Figure 4b). In the case of **WP6**⊃**G2**/MWNT complexes, the hydrophobic section containing the pyrenyl ring attached to the surface of the MWNT, and the hydrophilic part containing the alkyl chain was included in the cavity of **WP6** dispersed in the water. Therefore, well dispersed MWNTs were distinguished (Figure 4c). SEM images of individual nanotubes (Figure S28) were in good agreement with the above TEM results.

To confirm the complexation between MWNTs and the **WP6**⊃**G2** host–guest complex, fluorescence spectroscopy was employed to compare the difference in fluorescence emission between the solution of **WP6**⊃**G2** and the aqueous dispersion of MWNTs. As shown in Figure S29, a solution of **WP6**⊃**G2** displayed characteristic fluorescence emission of pyrenyl groups with high intensity. However, after MWNTs were dispersed in that solution, strong fluorescence quenching was observed. As previously reported, when pyrene is bound to a CNT through  $\pi$ – $\pi$  stacking, it suffers fluorescence quenching as a result of energy transfer from pyrene to the CNT.<sup>11b</sup> Since the only difference between the solution of **WP6**⊃**G2** and the dispersion of MWNTs was the introduction of MWNTs, the quenching is attributed to **WP6**⊃**G2**–MWNT interactions.

Additional proof for **WP6**⊃**G2**–MWNT interactions came from UV–vis–NIR spectra of **WP6**⊃**G2**/MWNT complexes (Figure S30). Upon addition of a **WP6**⊃**G2** solution (molar ratio 1:1), the absorbance range from 600 to 900 nm corresponding to the characteristic absorptions of CNTs increased gradually.<sup>11d</sup> Usually these absorptions are not observable because of the poor solubility of CNTs. Upon addition of **WP6**⊃**G2**, the appearance of the characteristic absorptions of CNTs clearly indicated the homogeneous dispersion of the MWNTs in aqueous solution.

Moreover, we employed thermogravimetric analysis to see whether the **WP6**⊃**G2** host–guest complex modified the MWNTs and to calculate the content of **WP6**⊃**G2** in the system (Figure S31). **WP6**⊃**G2**/MWNT hybrids were prepared by sonication of **WP6**⊃**G2** (20 mg, 0.009 mmol) in  $\text{H}_2\text{O}$  (5 mL) with 1 mg of MWNTs. During the sonication, the aqueous solution changed from colorless to black, indicating solubilization of MWNTs. After the sonication, insoluble MWNTs were

removed by centrifugation. The supernatant was dialyzed against H<sub>2</sub>O for 2 weeks to remove excess free WP6G2 from the solution. Another sample of the original untreated MWNTs was also studied as a control experiment. Compared with the original MWNTs, the prepared sample of WP6G2/MWNTs underwent 44.6% weight loss up to 650 °C, corresponding to the decomposition temperature of MWNTs, which provided additional evidence of the interaction between WP6G2 and MWNTs. These results indicate that WP6G2 has a strong ability to keep MWNTs well-dispersed for a long time, and the solubility of MWNTs can be reversibly controlled.

In summary, we have successfully synthesized the first water-soluble pillar[6]arene. In contrast to the tubular aggregates formed by amphiphilic molecule G1, the host-guest complex WP6G1 self-assembled into vesicles. The reversible transformation between nanotubes and vesicles could be easily controlled by changing the pH. Furthermore, the confined hydrophobic cavity of WP6 could be utilized to interact with a neutral guest containing a pyrenyl group. This host-guest complex can be used in the pH-controlled reversible dispersion of MWNTs in water. The new recognition motif based on the water-soluble pillar[6]arene has potential applications in many fields, including supramolecular polymers, nanoelectronics, sensors, and drug and gene delivery systems.

## ■ ASSOCIATED CONTENT

### Supporting Information

Experimental details and supporting data. This material is available free of charge via the Internet at <http://pubs.acs.org>.

## ■ AUTHOR INFORMATION

### Corresponding Author

fhuang@zju.edu.cn

### Notes

The authors declare no competing financial interest.

## ■ ACKNOWLEDGMENTS

This work was supported by the National Natural Science Foundation of China (20834004, 91027006, 21125417), the Fundamental Research Funds for the Central Universities (2012QNA3013), the Program for New Century Excellent Talents in University, and the Zhejiang Provincial Natural Science Foundation of China (R4100009).

## ■ REFERENCES

- (1) (a) Davidson, G. J. E.; Loeb, S. J. *Angew. Chem., Int. Ed.* **2003**, *42*, 74. (b) Huang, F.; Nagvekar, D. S.; Slebodnick, C.; Gibson, H. W. *J. Am. Chem. Soc.* **2005**, *127*, 484. (c) Huang, F.; Lam, M.; Mahan, E. J.; Rheingold, A. L.; Gibson, H. W. *Chem. Commun.* **2005**, 3268. (d) Liu, Y.; Bruneau, A.; He, J.; Abliz, Z. *Org. Lett.* **2008**, *10*, 765. (e) Niu, Z.; Gibson, H. W. *Chem. Rev.* **2009**, *109*, 6024. (f) Davidson, G. J. E.; Sharma, S.; Loeb, S. J. *Angew. Chem., Int. Ed.* **2010**, *49*, 4938. (g) Jiang, W.; Schäfer, A.; Mohr, P. C.; Schalley, C. A. *J. Am. Chem. Soc.* **2010**, *132*, 2309. (h) Niu, Z.; Huang, F.; Gibson, H. W. *J. Am. Chem. Soc.* **2011**, *133*, 2836. (i) Zhu, K.; Vukotic, V. N.; Loeb, S. J. *Angew. Chem., Int. Ed.* **2012**, *51*, 2168. (j) Qi, Z.; Molina, P. M.; Jiang, W.; Wang, Q.; Nowosinski, K.; Schulz, A.; Gradzielski, M.; Schalley, C. A. *Chem. Sci.* **2012**, *3*, 2073. (k) Zheng, B.; Wang, F.; Dong, S.; Huang, F. *Chem. Soc. Rev.* **2012**, *41*, 1621.
- (2) (a) Mirzoian, A.; Kaifer, A. E. *Chem. Commun.* **1999**, 1603. (b) Liao, X. J.; Chen, G. S.; Liu, X. X.; Chen, W. X.; Chen, F. E.; Jiang, M. *Angew. Chem., Int. Ed.* **2010**, *49*, 4409.
- (3) Philip, I. E.; Kaifer, A. E. *J. Am. Chem. Soc.* **2002**, *124*, 12678.
- (4) (a) Gómez-Kaifer, W.; Ong, M.; Kaifer, A. E. *Org. Lett.* **2002**, *4*, 1791. (b) Jeon, Y. J.; Kim, H.; Jon, S.; Selvapalam, N.; Seo, D. H.; Oh, I.; Park, C.-S.; Jung, S. R.; Koh, D.-S.; Kim, K. *J. Am. Chem. Soc.* **2004**, *126*, 15944.
- (5) (a) Lehn, J.-M. *Supramolecular Chemistry*; VCH: Weinheim, Germany, 1995. (b) Sauvage, J.-P. *Acc. Chem. Res.* **1998**, *31*, 611. (c) Armaroli, N.; Balzani, V.; Collin, J.-P.; Gaviña, P.; Sauvage, J.-P.; Ventura, B. *J. Am. Chem. Soc.* **1999**, *121*, 4397. (d) Collin, J.-P.; Dietrich-Buchecker, C.; Gaviña, P.; Jimenez-Molero, M. C.; Sauvage, J.-P. *Acc. Chem. Res.* **2001**, *34*, 477. (e) Huang, F.; Fronczek, F. R.; Gibson, H. W. *J. Am. Chem. Soc.* **2003**, *125*, 9272. (f) Huang, F.; Gibson, H. W. *J. Am. Chem. Soc.* **2004**, *126*, 14738. (g) Jonkheijm, P.; Meijer, E. W. *Science* **2006**, *313*, 80. (h) Kay, E. R.; Leigh, D. A.; Zerbetto, F. *Angew. Chem., Int. Ed.* **2007**, *46*, 72. (i) Wang, C.; Yin, S.; Chen, S.; Xu, H.; Wang, Z.; Zhang, X. *Angew. Chem., Int. Ed.* **2008**, *47*, 9049. (j) Wang, F.; Zhang, J.; Ding, X.; Dong, S.; Liu, M.; Zheng, B.; Li, S.; Wu, L.; Yu, Y.; Gibson, H. W.; Huang, F. *Angew. Chem., Int. Ed.* **2010**, *49*, 1090. (k) Yan, X.; Wang, F.; Zheng, B.; Huang, F. *Chem. Soc. Rev.* **2012**, DOI: 10.1039/C2CS35091B.
- (6) (a) Ogoshi, T.; Kanai, S.; Fujinami, S.; Yamagishi, T. A.; Nakamoto, Y. *J. Am. Chem. Soc.* **2008**, *130*, 5022. (b) Zhang, Z.; Xia, B.; Han, C.; Yu, Y.; Huang, F. *Org. Lett.* **2010**, *12*, 2385. (c) Ogoshi, T.; Hashizume, M.; Yamagishi, T.; Nakamoto, Y. *Chem. Commun.* **2010**, 46, 3708. (d) Li, C.; Zhao, L.; Li, J.; Ding, X.; Chen, S.; Zhang, Q.; Yu, Y.; Jia, X. *Chem. Commun.* **2010**, 46, 9016. (e) Zhang, Z.; Yu, G.; Han, C.; Liu, J.; Ding, X.; Yu, Y.; Huang, F. *Org. Lett.* **2011**, *13*, 4818. (f) Zhang, Z.; Luo, Y.; Chen, J.; Dong, S.; Yu, Y.; Ma, Z.; Huang, F. *Angew. Chem., Int. Ed.* **2011**, *50*, 1397. (g) Zhang, Z.; Luo, Y.; Xia, B.; Han, C.; Yu, Y.; Chen, X.; Huang, F. *Chem. Commun.* **2011**, 47, 2417. (h) Strutt, N. L.; Forgan, R. S.; Spruell, J. M.; Botros, Y. Y.; Stoddart, J. F. *J. Am. Chem. Soc.* **2011**, *133*, 5668. (i) Hu, X.-B.; Chen, L.; Si, W.; Yu, Y.; Hou, J.-L. *Chem. Commun.* **2011**, 47, 4694. (j) Li, C.; Chen, S.; Li, J.; Han, K.; Xu, M.; Hu, B.; Yu, Y.; Jia, X. *Chem. Commun.* **2011**, 47, 11294. (k) Ma, Y.; Ji, X.; Xiang, F.; Chi, X.; Han, C.; He, J.; Abliz, Z.; Chen, W.; Huang, F. *Chem. Commun.* **2011**, 47, 12340. (l) Cragg, P. J.; Sharma, K. *Chem. Soc. Rev.* **2012**, *41*, 597. (m) Hu, X.-Y.; Zhang, P.; Wu, X.; Xia, W.; Xiao, T.; Jiang, J.; Lin, C.; Wang, L. *Polym. Chem.* **2012**, DOI: 10.1039/C2PY20285A. (n) Xue, M.; Yang, Y.; Chi, X.; Zhang, Z.; Huang, F. *Acc. Chem. Res.* **2012**, DOI: 10.1021/ar2003418.
- (7) (a) Cao, D.; Kou, Y.; Liang, J.; Chen, Z.; Wang, L.; Meier, H. *Angew. Chem., Int. Ed.* **2009**, *48*, 9721. (b) Han, C.; Ma, F.; Zhang, Z.; Xia, B.; Yu, Y.; Huang, F. *Org. Lett.* **2010**, *12*, 4360. (c) Ma, Y.; Zhang, Z.; Ji, X.; Han, C.; He, J.; Abliz, Z.; Chen, W.; Huang, F. *Eur. J. Org. Chem.* **2011**, 5331. (d) Yu, G.; Han, C.; Zhang, Z.; Chen, J.; Yan, X.; Zheng, B.; Liu, S.; Huang, F. *J. Am. Chem. Soc.* **2012**, *134*, 8711. (e) Ma, Y.; Chi, X.; Yan, X.; Liu, J.; Yao, Y.; Chen, W.; Huang, F.; Hou, J.-L. *Org. Lett.* **2012**, *14*, 1532.
- (8) Kulasekharan, R.; Ramamurthy, V. *Org. Lett.* **2011**, *13*, 5092.
- (9) Kasha, M.; Rawls, H. R. *Pure Appl. Chem.* **1965**, *11*, 371.
- (10) (a) Naka, K.; Chujo, Y. *Langmuir* **2003**, *19*, 5496. (b) Shimazaki, Y.; Yamamoto, M. *Langmuir* **1997**, *13*, 1385.
- (11) (a) Guldi, D. M.; Rahman, G. M. A.; Jux, N.; Balbinot, D.; Hartnagel, U.; Tagmatarchis, N.; Prato, M. *J. Am. Chem. Soc.* **2005**, *127*, 9830. (b) Guldi, D. M.; Rahman, G. M. A.; Zerbetto, F.; Prato, M. *Acc. Chem. Res.* **2005**, *38*, 871. (c) Ogoshi, T.; Takashima, Y.; Yamaguchi, H.; Harada, A. *J. Am. Chem. Soc.* **2007**, *129*, 4748. (d) Chen, S.; Jiang, Y.; Wang, Z.; Zhang, X.; Dai, L.; Smet, M. *Langmuir* **2008**, *24*, 9233. (e) Ding, Y.; Chen, S.; Xu, H.; Wang, Z.; Zhang, X. *Langmuir* **2010**, *26*, 16667. (f) Wang, X.; Wang, C.; Cheng, L.; Lee, S.-T.; Liu, Z. *J. Am. Chem. Soc.* **2012**, *134*, 7414.
- (12) (a) Star, A.; Stoddart, J. F. *Macromolecules* **2002**, *35*, 7516. (b) Star, A.; Liu, Y.; Grant, K.; Ridvan, L.; Stoddart, J. F.; Steuerman, D. W.; Diehl, M. R.; Boukai, A.; Heath, J. R. *Macromolecules* **2003**, *36*, 553.
- (13) Keizer, J. *J. Am. Chem. Soc.* **1983**, *105*, 1494.